is of theoretical interest since it may signal a change in the order of the γ transition with chain length as γ and α merge.[31]

Summary and Conclusions

We have studied the solid–solid phase transitions in the odd *n*-alkanes C_{17}–C_{29} using DSC and IR spectroscopy. The major results are summarized as follows:

(1) The odd *n*-alkanes, C_{17}–C_{23}, exhibit a single solid–solid phase transition, which has been previously reported.[7] However, C_{25}–C_{29} exhibit two additional phase transitions which were detected by DSC measurements. These latter transitions are correlated with transitions recently reported[16,17] for *n*-alkanes longer than C_{29} (Figure 1).

(2) At *every* phase transition detected by DSC, we have observed discontinuous changes in the infrared spectra. These changes result from abrupt increases in the concentrations of nonplanar conformations.

(3) The nature of the nonplanar conformations found in the solid phases of the *n*-alkanes is quite different from that in the liquid state. In the highest-temperature solid phase (II), three specific nonplanar defects were identified. These are the "end-gauche", "kink", and "double-gauche" forms. The end-gauche and kink forms are the dominant nonplanar conformers present in phase II. The double-gauche defects occur in much lower concentrations than the others although very near the melting point their concentration increases markedly.

(4) The concentrations of nonplanar conformers increase roughly linearly with increasing chain length. For C_{27} and C_{29}, the longest chains studied, we estimate that end-gauche defects occur in ~20–30% of the molecules while kink defects occur in ~60–70% of the molecules.

(5) The formation of end-gauche defects is a disordering process that is common to all of the phase transitions. Kink defects, on the other hand, seem to be formed primarily (or exclusively) at the α transition.

(6) The concentration of defects increases with increasing temperature within each phase. This increase is greatest in the highest-temperature phase as the melting point is approached but occurs in other phases as well.

(7) The sharpness of the γ transition appears to be dependent on the temperature separation between T_γ and T_α which in turn is a function of chain length. This behavior may result from some type of "interaction" between the α and γ transitions.

We return to the question raised in the Introduction—how is the defect structure of the alkane chains related to the existence of distinct solid phases? The phase diagram (Figure 1) shows an increasing number of phases as the chain length increases. We have shown that the number of defects also increases rapidly as a function of chain length until most of the chains of C_{29} are nonplanar in the highest-temperature phase. This suggests that the conformational disorder is intimately linked with the very existence of the many phases transitions. The older concept of a "rotator" phase is too simple and, in fact, for the longer chains the kink-block model[14] may be a more appropriate starting point for describing the highest-temperature phase.

It is difficult to envision the distinct kinds of long-range order that must be characteristic of the many solid phases. There seem to be some analogies to liquid crystal smectic B phases,[32] which have a layer structure with order in each layer. Various models which are either more crystallike or more liquidlike are discussed in ref 32. We emphasize that for the *n*-alkanes we need to account for at least four phases intermediate between the low-temperature solid and the liquid. The existence of these subtle ordering phenomena presents many opportunities for further study. They suggest the possibility of arriving at an overall description of "order" in *n*-alkane systems which would elucidate the structure of many chain assemblies of vital importance.

Acknowledgment. We gratefully acknowledge support from the National Institutes of Health and the National Science Foundation. M.M. has been sponsored as a Chevron Chemistry Fellow.

Registry No. *n*-$C_{19}H_{40}$, 629-92-5; *n*-$C_{21}H_{44}$, 629-94-7; *n*-$C_{23}H_{48}$, 638-67-5; *n*-$C_{25}H_{52}$, 629-99-2; *n*-$C_{27}H_{56}$, 593-49-7; *n*-$C_{29}H_{60}$, 630-03-5; *n*-$C_{16}H_{34}$, 544-76-3; *n*-$C_{17}H_{36}$, 629-78-7.

(31) The presence of impurities can also lead to a broadening of these transitions (see ref 17). The fact that the changes are systematic with chain length, that we observe the weak δ transition, and that the α transition is sharp for C_{27}, however, argues against this possibility.

(32) P. G. deGennes, "The Physics of Liquid Crystals", Oxford University Press, Oxford, 1974.

Influence of Ion Pairing on Cation Transport in the Polymer Electrolytes Formed by Poly(ethylene oxide) with Sodium Tetrafluoroborate and Sodium Tetrahydroborate

R. Dupon,[†] B. L. Papke,[†] M. A. Ratner,*[†] D. H. Whitmore,*[‡] and D. F. Shriver*[†]

Contribution from the Materials Research Center and Departments of Chemistry and Materials Science, Northwestern University, Evanston, Illinois 60201. *Received January 14, 1982*

Abstract: Vibrational spectroscopic and conductivity data for complexes of $NaBF_4$ and $NaBH_4$ with poly(ethylene oxide) indicate that extensive contact ion pairing occurs in the $NaBH_4$ complex but not in the $NaBF_4$ complex. As a result the ionic conductivity is considerably lower in the $NaBH_4$ complex due to trapping of the mobile sodium cations by the anion. Conductivity studies on mixed anion complexes of poly(ethylene oxide) containing both ion-pairing (BH_4^-) and non-ion-pairing (BF_4^-) anions suggest that cation transport in these systems is not limited by motion through the polymer helical channels in which the cation is thought to reside. Conduction between helical chains appears to be a dominant process.

Introduction

Solid materials which exhibit anomalously high ionic conductivity ($\sigma > 10^{-5}\ \Omega^{-1}\ cm^{-1}$) are referred to as fast-ion conductors or solid electrolytes. They are the topic of considerable current research both for applications to fuel cells, sensors, electrolytic cells, and high-energy-density batteries and because the mechanisms which lead to high ionic mobility in solids are of considerable intrinsic interest. Most solid electrolytes are either of framework type or of molten-sublattice type. The framework materials are hard, covalent solids (often silicates, titanates, or aluminas), which transport monocations such as Na^+, K^+, Ag^+, or Li^+. The

[†] Chemistry Department.
[‡] Materials Science Department.

0002-7863/82/1504-6247$01.25/0

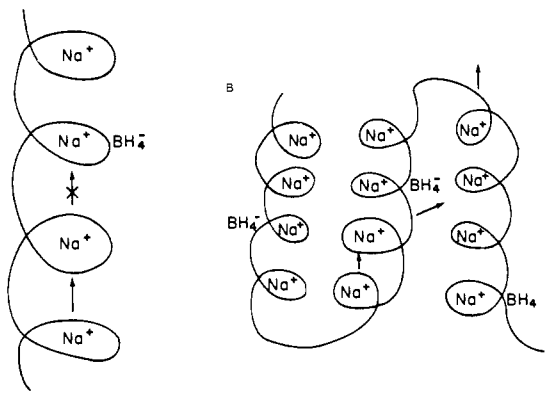

Figure 1. Schematic illustration of the influence of ion pairing on conductivity: (A) one-dimensional ion transport in helical tunnels is blocked by ion pairing with BH_4^-; (B) three-dimensional ion transport is not blocked by ion pairs.

molten-sublattice solid electrolytes are often heavy-metal halides, which undergo a phase transition of order–disorder type, at which the conductivity jumps significantly. Standard examples of the two classes are β'-alumina $(Na_2O)_x \cdot 11Al_2O_3$) and α-AgI, respectively.

Very recent work in several laboratories has been devoted to the conduction properties of polyether complexes of alkali-metal salts; these are solid electrolytes, are stable and compliant materials, and are quite promising as electrolytes in secondary cells. Complexes of poly(ethylene oxide) (PEO, $-(CH_2CH_2O)_n-$) with alkali-metal salts are known to exhibit reasonable ionic conductivities at moderate temperatures.[1-3] A structural model has been proposed for the approximately 70% crystalline Na^+ and Li^+ complexes in which the cation resides in a helical tunnel.[4-6] The cation has been implicated as a mobile species in the PEO·NaSCN complex through transference number measurements using a sodium/mercury amalgam concentration cell.[7] Vibrational spectroscopic and conductivity studies are presented here which indicate that extensive contact ion pairing occurs in the PEO·$NaBH_4$ complex, resulting in a considerably lower ionic conductivity than that observed in other sodium salt complexes of PEO.

The spectroscopic observation of ion pairing in $NaBH_4$·PEO and the lower conductivity of this complex has led us to employ BH_4^- doping to test whether cation conduction in the helical tunnels dominates the conductivity response in these materials. As indicated schematically in Figure 1, the presence of small concentrations of blocking ion pairs should greatly reduce the conductivity if ion transport in the one-dimensional tunnels dominates. If, however, interchain hopping or conductivity in the amorphous regions dominates, then the doping of a good conductor such as $NaBF_4$·PEO with low levels of the poor conductor $NaBH_4$·PEO should not greatly lower the conductivity.

Experimental Section

Purification of the poly(ethylene oxide), average molecular weight 600 000 (Aldrich, approximately 60–70% crystalline), and preparation of the PEO·$NaBF_4$ complex has been described elsewhere.[4] Sodium borohydride was purified by recrystallization from liquid ammonia. The PEO·$NaBH_4$ complex was prepared by suspending films of pure PEO in a saturated isopropylamine/$NaBH_4$ solution. The isopropylamine (Aldrich, 99%) was refluxed over CaH_2 under dry N_2 and distilled directly into the reaction flask. The sealed flask was shaken and stored 1–2 days in the dark to allow complete complexation. The films were then washed several times with freshly distilled anhydrous isopropylamine and dried under vacuum (10^{-3} torr) at room temperature. Care was taken to exclude traces of water and the complexed films were handled by using standard inert atmosphere techniques. The stoichiometry of the PEO·$NaBH_4$ complex was determined by protolysis of the BH_4^- using aqueous HCl followed by *PVT* measurements of the evolved H_2. The fully complexed polymer:salt stoichiometry thus established is about 3.4:1 (ether oxygens:sodium cations).

The mixed anion PEO·$Na(BF_4)_{1-x}(BH_4)_x$ complexes were prepared by suspending a PEO·$NaBF_4$ film of 4:1 stoichiometry in a saturated $NaBF_4$/isopropylamine solution containing the desired amount of $NaBH_4$. An exchange occurs between the BH_4^- anions in solution and BF_4^- in the film; the saturated $NaBF_4$ solution prevents the films from losing any $NaBF_4$ aside from that replaced by $NaBH_4$. After several days in solution, the films were shaken free of solvent in a N_2-filled glovebag and dried under vacuum at room temperature. To prevent loss of $NaBF_4$, we did not wash the film. When they are prepared in this manner, microscopic examination of the mixed anion complexes indicates a homogeneous and highly crystalline material. In agreement with this interpretation the melting ranges of mixed materials are intermediate between that for the pure $NaBF_4$ complex (110 °C) and the $NaBH_4$ complex (175 °C). Microscopic examination through crossed Polaroids demonstrates complete and even extinction as the mixed anion complexes melt. This is followed by the crystallization of a pure PEO·$NaBH_4$ phase if the melt is held at temperatures below 170 °C. Both BF_4^- and BH_4^- vibrational bands were observed in the infrared for these complexes. Stoichiometry was determined by elemental analysis and comparison with the initial salt stoichiometry. The fully complexed polymer:total salt stoichiometries for the mixed anion systems were in every case intermediate between that of pure PEO·$NaBH_4$ (3.4:1) and PEO·$NaBF_4$ (4:1) (ether oxygens:sodium cations).

Optical microscopic examinations of each system studied revealed spherulitic morphology for the crystallites. Glass transition temperatures for both pure complexes were determined by differential scanning calorimetry to be in the range −20 to −15 °C (T_g for pure PEO is −60 °C). All of the complexes were anhydrous, as determined by the absence of infrared bands at ca. 3400 and 1610 cm^{-1}. The complexes were characterized by infrared and Raman spectroscopy, differential scanning calorimetry, optical microscopy using a hot stage polarized microscope, and X-ray diffraction. Conductivities were measured on pressed pellets of the polymer complex by using complex admittance/impedance techniques over the frequency range 5 Hz to 500 kHz. A Hewlett-Packard 4800A vector impedance meter was used. Ion-reversible sodium/mercury amalgam liquid electrodes were used as electrical contacts in a sealed cell.[7]

Results and Discussion

Spectroscopic Evidence for Ion Pairing in the PEO·$NaBH_4$. Vibrational spectroscopic techniques have been used to deduce a reasonable polyether conformation for the semicrystalline PEO·NaX complexes.[4] The polyether chain is believed to wrap around the sodium cations in a trans (CC–OC), trans (CO–CC), gauche (OC–CO), trans (CC–OC), trans (CO–CC), gauche-minus (OC–CO) conformation ($T_2GT_2\bar{G}$). The oxygen atoms are all directed inward in this helical conformation to coordinate the sodium cations in a pseudotetrahedral geometry. The PEO·$NaBH_4$ and PEO·$NaBF_4$ complexes have virtually identical conformations as determined by spectroscopic studies.

The internal vibrational modes of the BH_4^- and BF_4^- anions provide a convenient and powerful spectroscopic probe to study the local environment about the anion. The PEO·$NaBH_4$ (BD_4) complexes have B–H or B–D stretching vibrations in regions where PEO vibrational bands do not interfere. These are high-frequency bands centered around 2250 and 1650 cm^{-1}, respectively, and are easily perturbed by changes in environment and symmetry of the anion. The B–F stretching vibrations are buried in the infrared beneath intense C–O–C asymmetric stretching bands at about 1100 cm^{-1}. However, deformation modes at lower frequencies combined with far-infrared data are sufficient to monitor ion pairing here as well. If no cation–anion interactions occur, the internal vibrational bands observed for the polatomic anion should correspond closely to those for an unperturbed "free-ion" symmetry, in this case an anion of tetrahedral (T_d) symmetry. Significant cation–anion interactions would result in a lower symmetry

(1) Wright, P. V. *Br. Polym. J.* **1976**, *7*, 319.
(2) Armand, M. B., Chabagno, J. M.; Duclot, M. J. In "Fast Ion Transport in Solids"; Vashishta, P., Mundy, J. N., Shenoy, G. K., Eds.; North-Holland Publishing Co.: New York, 1979; pp 131–6.
(3) For a review of polymer electrolytes see: Shriver, D. F.; Papke, B. L.; Ratner, M. A.; Dupon, R.; Wong, T.; Brodwin, M. *Solid State Ionics* **1981**, *5*, 83.
(4) Papke, B. L.; Ratner, M. A.; Shriver, D. F. *J. Phys. Chem. Solids* **1981**, *42*, 493.
(5) Papke, B. L.; Ratner, M. A.; Shriver, D. F. *J. Electrochem. Soc.* **1982**, *129*, 1694.
(6) A double-helical model is proposed by: Parker, J. M.; Wright, P. V.; Lee, C. C. *Polymer* **1981**, *22*, 1305.
(7) Dupon, R.; Whitmore, D. H.; Shriver, D. F. *J. Electrochem. Soc.* **1981**, *128*, 715.

Table I. Infrared and Raman Vibrational Assignments for the BH_4^- Anion[a]

PEO·$NaBH_4$		$NaBH_4$ in basic aqueous solution		approx assignments
Raman	IR	Raman	IR	
		2460 w, p		$2\nu_4$
2342 w, sh	2347 vs	2340 w, p		$\nu_2 + \nu_4$
2313 vs	2295 m	2294 s, p		ν_1
		2266 w, dp	2272 s	ν_3
2230 w, b	2232 vs			ν_3
		2196 w, dp	2200 sh	$2\nu_4$ (E or F_2)
2177 m, sh	2178 s			
	2169 s			
2155 ms				
		2146 m, p		$2\nu_4$ (A_1)
		1246 w		ν_2
		1097 w		ν_4

[a] Band intensities: vw (very weak), w (weak), sh (shoulder), mw (medium weak), m (medium), ms (medium strong), s (strong), vs (very strong), b (broad), p (polarized), dp (depolarized).

Table II. Infrared and Raman Vibrational Assignments for the BD_4^- Anion[a]

PEO·$NaBD_4$		$NaBD_4$ in basic aqueous solution		approx assignments
Raman	IR	Raman	IR	
1750 sh	1751 vs			$\nu_2 + \nu_4$ (?)
1730 m	1731 vs			$\nu_2 + \nu_4$ (?)
		1723 w, dp	1721 s	ν_3
1713 m	1710 w			
		1694 m, p		$2\nu_4$ (A_1)
	1684 s			
	1679 s			
		1675 w, dp	1666 sh	$2\nu_4$ (E or F_2)
1653 w	1650 sh			
1638 w	1639 s			
1578 s	1579 m	1585 s, p		ν_1
	947 vw	890 w		ν_2
	853 mw			ν_4
	830 m	842 vw	843 w	ν_4

[a] Band intensities: vw (very weak), w (weak), sh (shoulder), mw (medium weak), m (medium), ms (medium strong), s (strong), vs (very strong), b (broad), p (polarized), dp (depolarized).

accompanied by the observation of new bands owing to splitting of degenerate vibrational modes, and general relaxation of the selection rules.

The aqueous BH_4^- (BD_4^-) anion is representative of the unperturbed anion; its vibrational frequencies and assignments are shown in Tables I and II. Only the triply degenerate modes, ν_3 and ν_4, respectively, are formally infrared active and Fermi resonance has been invoked to explain the position of the totally symmetric $\nu_1(A_1)$ stretching mode.[8] In contrast, the BH_4^- (BD_4^-) vibrational band structures for the PEO complexes are rather complex. From a comparison of the number and intensity of the vibrational bands indicated in Tables I and II, it is clear that the symmetry of the BH_4^- (BD_4^-) anion has been lowered from tetrahedral. For example, vibrational bands which are normally expected to be degenerate in a T_d symmetry, such as $\nu_4(F_2)$, are no longer degenerate in the PEO complexes, and the large number of vibrational bands observed in the B–H and B–D stretching regions (2150–2450 or 1570–1750 cm^{-1}, respectively) are due in part to lifting of degeneracies.

Qualitatively the B–H or B–D stretching regions of these complexes have Raman spectra similar to those reported by Shirk and Shriver for basic aqueous solutions of $NaBH_4$ or $NaBD_4$.[8] When compared with infrared data, however, the picture becomes more complex. A total of seven bands are observed in the B–H stretching region and eight bands in the B–D stretching region, and only small changes in intensity or band position occur between 110 and −150 °C in the infrared. Symmetric and asymmetric deformation modes for BH_4^- and BD_4^- are weak and often buried beneath PEO bands. A few deformation bands were identified through careful comparison of spectra for BH_4^- and BD_4^- complexes and are indicated in Tables I and II. The complexity of bands observed in B–H and B–D stretching regions and masking of anion deformation bands make it impractical to give complete assignments for the BH_4^- or BD_4^- bands, but comparison with Raman and infrared spectra for the $NaBH_4$ or $NaBD_4$ salts in solution provides some provisional assignments.

The BH_4^- anion may interact with a PEO-complexed cation in several ways. One possible interaction is through a single B–H bond, resulting in a C_{3v} anion symmetry; another possibility is through two B–H bonds (C_{2v} symmetry). Accidental overlapping of bands and Fermi resonance undoubtedly complicate the BH_4^- and BD_4^- spectra in these complexes, and either anion symmetry is possible. Since the actual anion symmetry in the complex is unknown, the discussion will relate the observed bands of the perturbed BH_4^- ions to those found for the tetrahedral (T_d) symmetry of unperturbed BH_4^- anions.

In Raman studies of BH_4^- in various solvents, the $\nu_1(A_1)$ totally symmetric stretching mode is the most intense band, and, when Fermi resonance is not strong, the frequency range is generally 2280–2306 cm^{-1}.[7] For solutions containing BD_4^-, the $\nu_1(A_1)$ mode is observed between 1570 and 1590 cm^{-1}. Often this low frequency results from Fermi resonance with A_1 components of $2\nu_4$.[9] A single intense Raman-active band is present with the same frequency ranges for PEO·$NaBH_4(BD_4)$ complexes, at 2313 cm^{-1} (1578), and is believed to derive from the $\nu_1(A_1)$ mode. The existence of the BH_4^- anions in different local environments within the PEO complex could account for the complex band structure. However, the existence of a single band attributable to the $\nu_1(A_1)$ mode, which is particularly sensitive to local environment, indicates only one type of anion site.[8]

The asymmetric stretching mode, $\nu_3(F_2)$, is typically the strongest infrared-active band, observed around 2200–2270 cm^{-1} for BH_4^-. This mode is triply degenerate for T_d symmetry, and a strong infrared band at 2232 cm^{-1} for PEO·$NaBH_4$ is assigned to at least one component of this mode. A more complicated situation exists for PEO·$NaBD_4$ complexes and preliminary assignments for $\nu_3(F_2)$ modes have not been made.

Tentative assignments for $\nu_2(E)$ and $\nu_4(F_2)$ derived modes in PEO·$NaBD_4$ complexes are indicated in Table II. Through a careful comparison of infrared spectra for PEO·$NaBH_4$ and PEO·$NaBD_4$ complexes, two medium to weak bands at 830 and 853 cm^{-1} in the PEO·$NaBD_4$ complex can be assigned to modes derived from the $\nu_4(F_2)$ mode of tetrahedral BD_4^-. A very weak Raman-active band at 947 cm^{-1} is thought to derive from the $\nu_2(E)$ mode of BD_4^-.

In contrast, the BF_4^- anion in PEO·$NaBF_4$ retains nearly tetrahedral symmetry. Raman-active vibrational bands for the anion are essentially identical with those for aqueous $NaBF_4$ solutions or molten $NaBF_4$,[10] for which a tetrahedral symmetry has been proposed. No lifting of degeneracy is observed in the vibrational spectra of PEO·$NaBF_4$ complexes, and the only indication of small perturbations from tetrahedral symmetry is the presence of a medium-intensity infrared-active band at 765 cm^{-1}. This is assigned to the $\nu_1(A_1)$ mode and is formally infrared inactive for a strictly T_d symmetry.

The best explanation for the complexity of observed anion vibrational bands for PEO·$NaBH_4(BD_4)$ complexes is that ion-pair interactions have perturbed the T_d symmetry. Far-infrared observations support the hypothesis of cation–anion-pair interactions as well. Cation-dependent far-infrared vibrational bands, corresponding to a cage-type motion of the alkali-metal cations relative to counteranions and surrounding ether oxygens, have been observed for the PEO complexes.[3,4] A number of the PEO·NaX

(8) Shirk, A. E.; Shriver, D. F. *J. Am. Chem. Soc.* **1973**, *95*, 5901.

(9) Emery, A. R.; Taylor, R. C. *J. Chem. Phys.* **1958**, *28*, 1029.

(10) Quist, A. S.; Bates, J. B.; Boyd, G. F. *J. Chem. Phys.* **1971**, *54*, 4896.

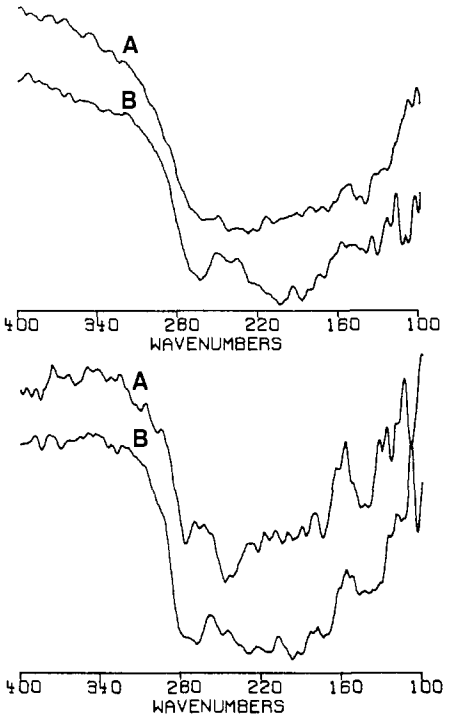

Figure 2. Comparison of far-infrared spectra for (A) PEO·$NaBH_4$ and (B) PEO·$NaBD_4$ complexes (upper spectra, room temperature; lower spectra, liquid-nitrogen temperature).

complexes, including PEO·$NaBF_4$, exhibit little anion dependence for their cation-cage modes, indicating that the anion resides outside the first coordination sphere of the cation. Several relatively sharp bands are observed in the far-infrared around 200 cm^{-1} for most of the PEO·NaX complexes. In contrast, band structures for the PEO·$NaBH_4$ and PEO·$NaBD_4$ complexes are rather broad in the far-infrared, and an anion dependence is observed (see Figure 2).

Influence of Ion Pairing on Conductivity. Several mechanistic possibilities for ion transport in these polymer materials can be envisaged. The simplest would involve ion hopping in the helical pipes and might be similar to ionic motion in tunnel-type framework ionic conductors such as β-eucryptite. This would imply simple Arrhenius behavior in the logarithmic conductivity–temperature plot, as well as characteristic and strong dependences on stoichiometry. A second mechanism, which has been used to explain transport and relaxation processes in fused salts, polymers, and other glass-forming materials, involves local, liquidlike motions of the solvent (polyether) with the ions then moving in an amorphous, locally disordered (liquid), environment. This picture implies curved plots, ln σT vs. $1/T$ over the entire temperature range with no discontinuities, much weaker stoichiometry dependence, and increase in conduction with decreased glass transition temperatures.[5] The PEO/NaX salts are generally highly crystalline and do not exhibit curved conductivity plots, so that the local-liquid picture seems questionable. Nevertheless, there are significant amorphous regions in these materials, and one can question the relative roles of motion in the helical and amorphous regions in determining the conductivity.

Strong ion pairing may effectively trap the mobile cations, significantly reducing the observed ionic conductivity relative to non-ion-paired complexes of similar structure. The non-ion-paired PEO·$NaBF_4$ complex at 4.5:1 stoichiometry exhibits an ionic conductivity similar to that reported for other semicrystalline sodium salt complexes at this stoichiometry.[2] In contrast, the 4.5:1 PEO·$NaBH_4$ complex has a much lower conductivity (by roughly a factor of 100) over the same temperature range (Figure 3). The knee observed at about 60 °C ($10^3/T = 3.0$) in the Arrhenius plots of the 4.5:1 complexes is attributed to the presence of small amounts of uncomplexed PEO (melting point = 55–60 °C) in these systems. The presence of uncomplexed PEO is substantiated

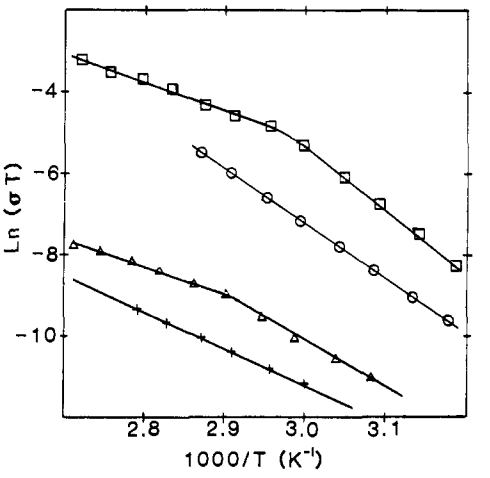

Figure 3. Variable-temperature conductivity values for PEO·$NaBF_4$ at 4.5:1 (□) and 3.1 (○) stoichiometry, and PEO·$NaBH_4$ at 4.5:1 (△) and 3.4:1 (+) stoichiometry.

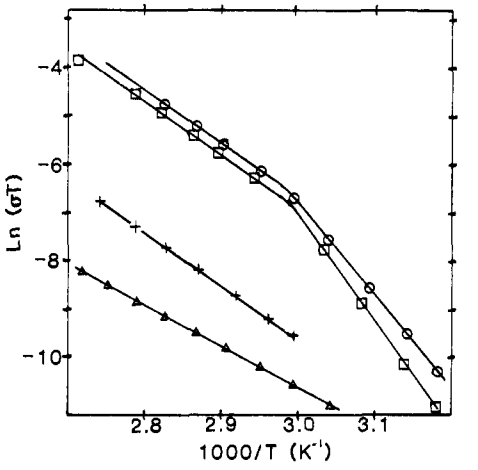

Figure 4. Variable-temperature conductivity values for PEO·$NaBF_4$ 4:1 (○), PEO·$NaBH_4$ 3.4:1 (△), and PEO·Na^+ (0.75 BF_4^- + 0.25BH_4^-) (□), and PEO·Na^+ (0.49BF_4^- + 0.51BH_4^-) (+).

by differential scanning calorimetry traces of complexes with varying PEO:salt ratios which reveal melting endotherms centered at 60 °C, the intensities of which diminish with increasing salt content. If a slight excess of $NaBF_4$ is present to ensure complete complexation (i.e., the nominal 3:1 PEO·$NaBF_4$ complex in Figure 3), the conductivity falls by a factor of 3 relative to the 4.5:1 stoichiometry. Likewise the conductivity of the fully complexed PEO·$NaBH_4$ material at 3.4:1 stoichiometry is lower than the 4.5:1 PEO·$NaBH_4$ complex, so the same relative separation in conductivities is maintained for the non-ion-paired $NaBF_4$ complex compared to the ion-paired $NaBH_4$ complex.

Ionic Conductivity Measurements on Mixed Anion Complexes. A method to probe possible ion conduction paths in the highly crystalline sodium salt complexes of PEO was suggested by results from the ion-pairing studies. Judging from infrared data the PEO·$NaBF_4$ and PEO·$NaBH_4$ complexes have nearly identical polymer backbone conformations; however, owing to ion pairing, the conductivity of the BH_4^- complex is ca. 100 times lower than that of BF_4^- complex for both systems at their fully complexed stoichiometries. A small amount of $NaBH_4$ statistically sufficient to block each chain segment in a mixed anion complex would be expected to limit the conductivity to that observed for a PEO·$NaBH_4$ complex if cation motion were restricted to helical channels. If cations can move from one chain to another, then the more mobile cation should be able to circumvent ion pairs which block the helix and the conductivity should fall only slowly with increasing BH_4^- content.

Variable-temperature conductivity plots for BH_4^--doped complexes are compared to pure PEO·$NaBF_4$ and PEO·$NaBH_4$

complexes in Figure 4. All of these complexes are near maximum stoichiometry. The results show only a gradual decrease in conductivity with increasing BH_4^- doping levels (Figure 3); even at 51% BH_4^- the observed conductivity is intermediate between that of pure PEO·$NaBH_4$ and PEO·$NaBF_4$ complexes. Thus, ion transport in crystalline regions of PEO·NaX complexes is not limited to cation motion along helical channels. Ion transport between chains, and/or in amorphous regions, dominates the conductivity in these materials. Transport would then occur by either associative (quintuply or triply coordinated Na^+ in the transition state) motion of the cation between stable quasi-tetrahedral coordination geometries. The motion can occur either within or between helical regions: if a helix is blocked, it can be circumvented by transfer of the cation to an amorphous region or to a neighboring helix.

Acknowledgment. This research was supported by the Office of Naval Research and by the NSF Materials Research Laboratory Program through the Northwestern Materials Research Center.

Peroxy Spin Probe Studies of Motion in Poly(vinylidene fluoride)

Darbha Suryanarayana and Larry Kevan*

Contribution from the Department of Chemistry, University of Houston, Houston, Texas 77004.
Received February 26, 1982

Abstract: Motional effects in poly(vinylidene fluoride) have been investigated using peroxy radicals as spin probes to contrast with previous studies of peroxy radical motion in polytetrafluoroethylene and in polyethylene. The predominant radical formed by radiolysis at 77 K is $-CF_2-CH_2$. In the presence of oxygen this radical readily converts to the peroxy radical $-CF_2-CH_2-O-O$. The electron spin resonance (ESR) spectrum of this peroxy radical was studied as a function of temperature from 77 to 360 K. The ESR spectrum measured at both 9 and 35 GHz revealed changes in the spectral line shapes due to averaging of the g anisotropy which is attributed to motion in this polymer. Various motional models including polymer chain-axis rotation, C–O bond rotation, and a cubic jump process were considered. The experimental variations in the spectra are best fit with a C–O bond rotation model with 180° jumps for a COO angle of 104° in a temperature range between 77 and 280 K. However, above 280 K extra lines between the $g_\parallel$ and $g_\perp$ regions of the spectra indicate that a cubic jump motional process dominates. This is presumably related to the greater freedom of motion at the higher temperature. The cubic jump motional process can be interpreted as a helical twisting motion of the end of a polymer chain.

Introduction

Peroxy radical formation is ubiquitous in irradiated polymers in the presence of oxygen and can easily be studied by electron spin resonance (ESR).[1] Peroxy radicals have been implicated in radiative and photooxydegradation processes of polymers. Not only must the chemistry of the peroxy radical be important in these polymer degradation processes, but also the types of internal motions of the peroxy radical site in the polymer framework must be of importance. Schlick and Kevan[2] have recently demonstrated that peroxy radicals are effective spin probes for elucidation of *specific* motional mechanisms in solids. It is possible to distinguish between rotation of the peroxy group around a C–O bond by a specific number of large angle jumps, cubic jump motion in which the g tensor of the peroxy radical is rotated around the body diagonal of a cube, and chain-axis rotation by large angle jumps in the case of polymeric systems. Two general classes of peroxy radicals may be formed in long-chain polymeric systems. One class consists of midchain peroxy radicals where the peroxy radical forms in the middle of the chain without breaking the carbon backbone. The other general class consists end-chain peroxy radicals in which a chain break occurs and the peroxy radical forms there. In a detailed study of peroxy radicals formed in γ-irradiated polytetrafluoroethylene it was found that both midchain and end-chain peroxy radicals could be studied independently. The temperature dependence of their ESR spectra indicated that the midchain peroxy radical principally undergoes cubic jump motion.[3] Peroxy radicals in polyethylene have been studied less completely, and the results indicate that either chain-axis rotation or C–O bond rotation motional mechanisms may be applicable,[4] although the most recent results suggest that chain-axis motion probably dominates for the midchain peroxy radicals in polyethylene.[5] On the other hand, when the polymer side groups can offer more steric hindrance to chain-axis motion such as in the methacrylates or in polypropylene, there is little evidence for chain-axis motion of the peroxy radicals formed in such polymers.[6]

Here we study the motion of peroxy radicals in poly(vinylidene fluoride) (PVF_2) and contrast the results to the cases of polyethylene and polytetrafluoroethylene. Although there appear to be few reports involving electron spin resonance studies of radicals produced in PVF_2,[7,8] there have been several recent reports on PVF_2 because of its net internal polarization.[9] This leads to a strong piezoelectricity,[10] pyroelectricity,[11] and interesting Brillouin scattering effects.[12] Thus the study of specific motional mechanisms as a function of temperature by the use of peroxy radical spin probes is not only of interest for comparison with other types of polymers but also because it may reveal information about the types of motion that are important in some of these effects due to the consequences of net polarization in the polymer.

(1) B. Ranby and J. F. Rabek, "ESR Spectroscopy in Polymer Research", Springer-Verlag, New York, 1977.
(2) S. Schlick and L. Kevan, *J. Phys. Chem.*, **83**, 3424 (1979).
(3) D. Suryanarayana, L. Kevan, and S. Schlick, *J. Am. Chem. Soc.*, in press.
(4) S. Schlick and L. Kevan, *J. Am. Chem. Soc.*, **102**, 4622 (1980).
(5) (a) Y. Hori, S. Shimada, and H. Ashiwabara, *Polymer*, **18**, 151, 567 (1977); (b) Y. Hori, S. Aoyama, and H. Kashiwabara, *J. Chem. Phys.*, **75**, 1582 (1981).
(6) D. Suryanarayana and L. Kevan, *J. Phys. Chem.*, **86**, 2042 (1982).
(7) J. N. Helbert, B. E. Wagner, E. H. Poindexter, and L. Kevan, *J. Polym. Sci., Part A-2*, **13**, 825 (1975).
(8) N. Tamura and K. Shinohara, *Rep. Progr. Polym. Phys. Jpn.*, **6**, 265 (1963).
(9) R. Hasegawa, M. Kobayashi, and H. Tadokoro, *Polym. J.*, **3**, 591 (1972).
(10) M. G. Broadhurst, G. T. Davis, J. E. McKinney, and R. E. Collins, *J. Appl. Phys.*, **49**, 4498 (1978).
(11) R. G. Pfister, M. Abkowitz, and R. G. Crystal, *J. Appl. Phys.*, **44**, 2064 (1973).
(12) C. H. Wang, D. B. Cavanaugh, and Y. Hagashigaki, *J. Polym. Sci.*, **19**, 941 (1981).

0002-7863/82/1504-6251$01.25/0